Title

Radially convergent groundwater flow in sloping terrain

Journal
Hydrological Sciences Journal, 51(4)

ISSN
0262-6667

Authors
LEIPNIK, ROY B
LOÁICIGA, HUGO A

Publication Date
2006-08-01

DOI
10.1623/hysj.51.4.700

Peer reviewed

Hydrological Sciences Journal

ISSN: 0262-6667 (Print) 2150-3435 (Online) Journal homepage: www.tandfonline.com/journals/thsj20

Radially convergent groundwater flow in sloping terrain

ROY B. LEIPNIK & HUGO A. LOÁICIGA

Radially convergent groundwater flow in sloping terrain

ROY B. LEIPNIK[1] **& HUGO A. LOÁICIGA**[2]

1 *Department of Mathematics, University of California, Santa Barbara, California 93106, USA*
leipnik@math.ucsb.edu

2 *Department of Geography, University of California, Santa Barbara, California 93106, USA*
hugo@geog.ucsb.edu

Abstract The groundwater flow equation governing the elevation (h) of the steady-state phreatic surface in a sloping aquifer fed by constant recharge over a bi-circular sector is $rhh' - r^2Bh' + Pr^2 - PR^2 = 0$, where r is the radial coordinate, P is a constant involving recharge and aquifer properties, and B is the slope of the aquifer–bedrock boundary. The derived flow equation describes radially convergent flow through a sloping aquifer that discharges to a water body of fixed head. One important simplification is that in which the width of the bi-circular sector is constant, and the draining land becomes a rectangular aquifer. The bi-circular sector and rectangular-strip groundwater flow problems are solved in terms of implicit equations. The solutions for the steady-state phreatic surfaces depend on the ratio of recharge to hydraulic conductivity, the slope of the aquifer–bedrock, and the downstream constant-head boundary. Computational examples illustrate the application of the solutions.

Key words aquifer recharge; hydraulic conductivity; ordinary differential equation; phreatic surface; unconfined flow

Ecoulement souterrain radialement convergent en terrain pentu

Résumé L'équation d'écoulement souterrain qui gouverne la cote (h) de la surface libre stabilisée d'un aquifère en pente alimenté par une recharge constante via un secteur bi-circulaire est $rhh' - r^2Bh' + Pr^2 - PR^2 = 0$, où r est la coordonnée radiale, P est une constante qui dépend de la recharge et de propriétés de l'aquifère, et B est la pente de l'interface aquifère–substrat. L'équation d'écoulement qui en est déduite décrit l'écoulement radialement convergent à travers un aquifère en pente qui s'écoule vers un exutoire d'altitude fixée. Le cas où la largeur du secteur bi-circulaire est constante et celui où l'aquifère est de forme rectangulaire sont deux cas simplificateurs importants. Les problèmes d'écoulement d'un secteur bi-circulaire et d'une nappe rectangulaire sont résolus au moyen d'équations implicites. Les solutions des surfaces libres stabilisées dépendent du rapport entre recharge et conductivité hydraulique, de la pente de l'interface aquifère–substrat et de la limite aval d'altitude fixe. Des exemples de calcul illustrent la mise en application des solutions.

Mots clefs recharge d'aquifère; conductivité hydraulique; équation différentielle ordinaire; surface libre; écoulement à surface libre

INTRODUCTION

The study of unconfined groundwater flow through sloping terrain owes its importance to the centrality that infiltration, aquifer recharge, and the ensuing perched phreatic surfaces have on runoff formation (Dunne, 1990; Smith, 2002; Cherkauer & Ansari, 2005; Loáiciga, 2005; Loáiciga & Huang, 2005). The geometry of phreatic surfaces in sloping aquifers is also useful in the calculation of groundwater discharge, in the analysis of slope stability, in the estimation of pore pressure created by perched groundwater, and its role on subsurface erosion (Terzaghi *et al.*, 1996; Coduto, 1999).

One situation of interest is that of a bi-circular sector of land that receives constant recharge (N) giving rise to unconfined groundwater discharging to a water body at the downstream end of the sloping terrain, see Fig. 1. A second situation arises when the tributary aquifer has a rectangular geometry as shown in Fig. 2. These two geometries of sloping unconfined aquifers were investigated by Dunne (1990), who wrote the governing equations for the height of the corresponding phreatic surfaces. No solutions were provided in Dunne (1990) for the sloping-aquifer case, however, and the case of

Open for discussion until 1 February 2007

the bi-circular-sector geometry remained unsolved in analytical form. Loáiciga (2005) presented implicit solutions for the case of sloping rectangular unconfined groundwater flow discharging to a stream or lake of constant water level h_0 (see Fig. 2).

This article presents, for the first time, the analytical solution for the geometry of steady-state phreatic surfaces created by constant recharge over bi-circular sectors of land discharging groundwater flow to a constant-head downstream boundary (see the pertinent geometry in Fig. 1). The results presented here include quantitative analysis of the factors governing the analytical solution. In addition, this work contains a comparison of the solution for the bi-circular-sector case to that pertinent to the rectangular-aquifer case (presented in Loáiciga, 2005) with the aim of contrasting similarities and differences among the two types of sloping unconfined groundwater flow.

GROUNDWATER FLOW EQUATION FOR A BI-CIRCULAR SECTOR

The steady-state groundwater flow at a distance r, $q(r)$, from the origin of the co-ordinate system in Fig. 1 equals the volumetric rate of recharge that accumulates in the area comprised between R and r (θ is the convergence angle of the bi-circular sector):

$$q(r) = \theta N \cdot \left(\frac{r^2 - R^2}{2} \right) \qquad r_s \le r \le R \tag{1}$$

The recharge rate N has units of volume per unit (horizontal) area of land and per unit time (i.e. length over time). Groundwater flow is directed towards the origin (where $r = 0$), hence the negative sign of $q(r)$ in equation (1). It follows from equation (1) that $q(R) = 0$. The groundwater flow reaches a maximum at $r = r_s$. There, the groundwater discharge per unit length of downstream boundary, $q'(r_s) \equiv q(r_s)/(r_s\,\theta)$, equals:

$$q'(r_s) = \frac{N}{2} \left(\frac{R^2 - r_s^2}{r_s} \right) \tag{2}$$

Equation (2) will prove useful in comparing radial groundwater discharge with groundwater discharge in a rectangular aquifer (see equation (29)).

The groundwater flow in equation (1) must equal that obtained by using Darcy's law, as follows (in which $h' = \mathrm{d}h/\mathrm{d}r$; $B \equiv \tan\beta$; K = hydraulic conductivity, and the Dupuit assumption of nearly horizontal streamlines is used):

$$\theta N \left(\frac{r^2 - R^2}{2} \right) = -K \cdot (h - rB) r\,\theta\,h' \tag{3}$$

The right-hand side of equation (3) implies that the groundwater flow may equal zero if (a) $h = rB$, in which case the saturated thickness is zero (this condition is implied in Fig. 1 at the location $r = R$, where $h(R) = RB$), or (b) $h'(r) = 0$, that is, the hydraulic gradient equals zero. Algebraic rearrangement of equation (3) produces the following equation governing the height of the phreatic surface under steady-state conditions (with $P \equiv N/(2K)$):

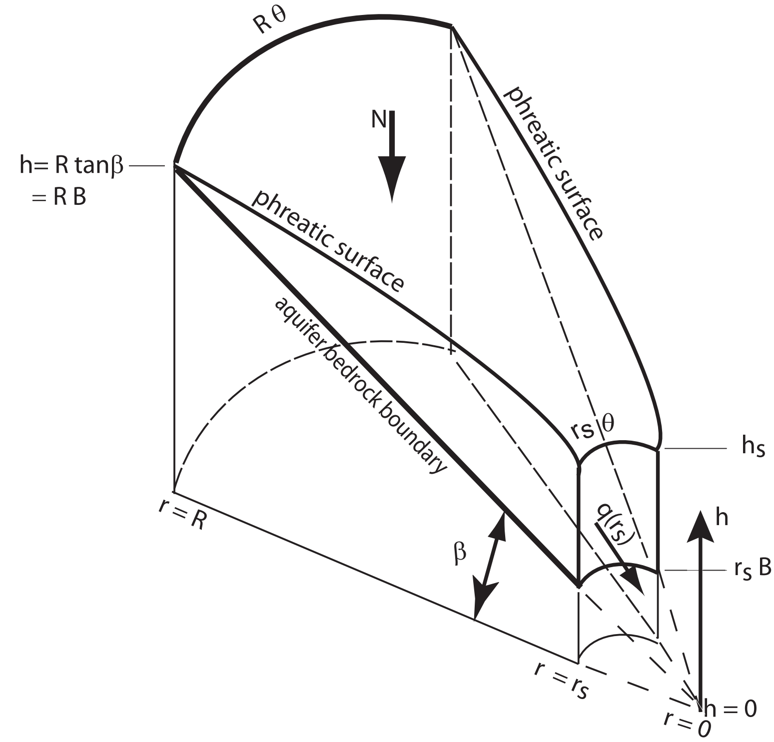

Fig. 1 Flow geometry in a bi-circular sector with convergence angle θ. The stream or lake are located at $r = r_s$, where the elevation of the phreatic surface equals h_s. See the text for other notation involved.

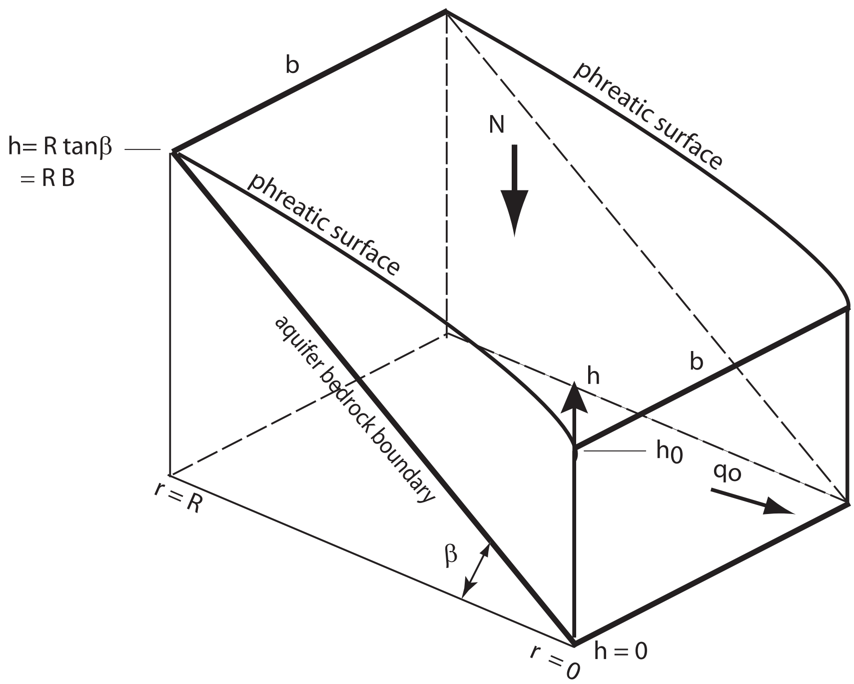

Fig. 2 Flow geometry in a rectangular strip of land of width b. The stream or lake are located at $r = 0$, where the elevation of the phreatic surface equals h_0. See the text for other notation involved.

$$r\,h\,h' - r^2\,B\,h' + P\,r^2 - P\,R^2 = 0 \qquad r_s \le r \le R \qquad h(r) \ge h_s \tag{4}$$

whose boundary condition is a constant head at $r = r_s$:

$$h(r_s) = h_s \tag{5}$$

The boundary head is specified so that $h_s < RB$ to induce groundwater flow downslope.

The hydraulic ratio $P = N/(2K)$ ranges between a minimum of 5×10^{-5} (corresponding to $N = 0.001$ m day^{-1} and $K = 10$ m day^{-1}) and 50 (when $N = 0.1$ m day^{-1} and $K = 0.001$ m day^{-1}), typically, in unconfined aquifers (Loáiciga, 2005). As for the aquifer slope, $0 < B \le 0.1$, so that the Dupuit assumption of nearly horizontal streamlines is well approximated.

The zero-slope case ($B = \tan\beta = 0$) leads to straightforward integration of equation (4) yielding:

$$h(r) = \left[2\,P\,R^2 \ln\left|\frac{r}{r_s}\right| - P\left(r^2 - r_s^2\right) + h_s^2 \right]^{\frac{1}{2}} \tag{6}$$

Equation (6) returns $h(r_s) = h_s$. Solution (6) describes the phreatic surface with recharge that would develop in a horizontal aquifer connecting two lakes separated by a distance $R - r_s$, one of which has elevation $h(R)$ and the other elevation h_s. Equation (6) will prove useful in the solution of the sloping-aquifer problem embodied by equations (4) and (5).

It is of mathematical and hydrologic significance that equation (4) is a special case of the Abel family of nonlinear ordinary differential equations (ODEs) of the form $(h + g(r))\,h' + f_2(r)\,h^2 + f_1(r)\,h + f_0(r) = 0$ (Abel, 1839), whose members appear frequently in mathematical physics (see, e.g. Kamke, 1959), and in hydrological diffusion processes (Polubarinova-Kochina, 1962; Philip, 1993; Loáiciga & Huang, 2005). The solution of this type of ODE is usually approximated numerically using Runge-Kutta algorithms. Much more can be learned, on the other hand, by deriving analytical solutions of the type derived in the remainder of this paper.

SOLUTION OF THE FLOW EQUATION THROUGH A BI-CIRCULAR SECTOR

Approaches to find analytical solutions to nonlinear differential equations rely on a variety of clever transformations and approximations (see, e.g. Kamke, 1959; Polyanin & Zaitsev, 1995). Infinite series sometimes prove successful for such tasks, as demonstrated in this work. Assume that the solution $h(r)$ of equations (4)–(5) satisfies the following expansion into infinite (implicit) series:

$$F(h,r) = \sum_{n=0}^{\infty} \left(h - h_s\right)^n \; f_n(r) = k \tag{7}$$

in which the weighting functions $f_n(r)$ and the constant k must be determined. Taking the derivative on both sides of equation (7) and noting that $\mathrm{d}F = (\partial F/\partial h)\mathrm{d}h + (\partial F/\partial r)\mathrm{d}r = \mathrm{d}k = 0$, produces the following result for the hydraulic gradient $h'(r)$

(letting $\mathrm{d}f_n/\mathrm{d}r = f'_n$):

$$h'(r) = -\frac{\sum_{n=0}^{\infty}\left(h-h_s\right)^n f'_n(r)}{\sum_{n=0}^{\infty} n\left(h-h_s\right)^{n-1} f_n(r)} \tag{8}$$

Substitution of equation (8) in the ODE (equation (4)) leads (using the identity $h - rB = h - h_s - (rB - h_s)$) to:

$$\sum_{n=0}^{\infty}\left(h-h_s\right)^{n+1} f'_n - \left(r\,B-h_s\right)\sum_{n=0}^{\infty}\left(h-h_s\right)^n f'_n + P\left(\frac{R^2}{r}-r\right)\sum_{n=0}^{\infty} n\left(h-h_s\right)^{n-1} f_n = 0 \tag{9}$$

The coefficients of $(h - h_s)^n$, $n = 0, 1, 2, 3, \ldots$, must equal zero for all values of $h - h_s$ if equation (9) is to hold. For $n = 0$ one obtains:

$$f_1\,P\cdot\left(\frac{R^2}{r}-r\right) = \left(r\,B-h_s\right)f'_0 \tag{10}$$

For $n = 1$:

$$f'_0 - \left(r\,B-h_s\right)f'_1 + P\cdot\left(\frac{R^2}{r}-r\right)2\,f_2 = 0 \tag{11}$$

The following recursion to generate the functions f_{n+1} is identified at once:

$$(n+1)\,f_{n+1}\cdot P\cdot\left(\frac{R^2}{r}-r\right) = \left(r\,B-h_s\right)f'_n - f'_{n-1} \tag{12}$$

for $n = 1, 2, 3, \ldots$, where f'_0 is required to start the recursion via equation (10) involving f_1 and f'_0.

Equation (7) implies that $F(h_s,r_s) = f_0(r_s) = k$. Furthermore, from the solution (6) for the case $B = 0$, let:

$$f_0(r) = \frac{h(r)^2}{2} = P\,R^2\ln\left|\frac{r}{r_s}\right| - \frac{P\,r^2}{2} + \frac{P\,r_s^2}{2} + \frac{h_s^2}{2} \tag{13}$$

with derivative:

$$f'_0 = P\cdot\left(\frac{R^2}{r}-r\right) \tag{14}$$

This implies, according to equation (10), that:

$$f_1(r) = r\,B - h_s \tag{15}$$

This choice imposes the following value of the constant k in the series (7):

$$F(h_s,r_s) = f_0(r_s) = \frac{h_s^2}{2} = k \tag{16}$$

The choice (13) for the starting weighting function $f_0(r)$ is not binding: others could be used (although $f_0(r)$ cannot equal a constant value). Equation (13), however, happens to lead to the relatively simple recursion (12) for $f_n(r)$, $n \geq 1$. It is appealing that it has a connection to the physically meaningful solution for phreatic surface when $B = 0$.

The solution to equations (4)–(5) is given in implicit form by the following power series:

$$F(h,r) = \sum_{n=0}^{\infty} \left(h(r) - h_s\right)^n f_n(r) = \frac{h_s^2}{2} \qquad r_s \leq r \leq R \qquad h(r) \geq h_s \tag{17}$$

with the functions $f_n(r)$ generated by equation (12), starting with $f_0(r)$ and $f_1(r)$ in equations (13) and (15), respectively.

Certain combinations of B and P render phreatic surfaces in which the head $h(r)$ falls in the interval (h_s, RB). This is, in fact, the situation graphed in Fig. 1. Other combinations produce heads $h > RB$. The latter situation arises when the aquifer–bedrock slope B is so small and/or P so large that the saturated thickness must take relatively large values to drain all the accruing recharge through the downstream boundary. The examples section illustrates the roles of B and P as controls of hydraulic head.

CONVERGENCE OF *F*(*h*, *r*) AND COMPUTATION OF *h*(*r*)

It can be shown that convergence of the power series in equation (17) requires that:

$$\left|\lambda_{1,2}\right| \left|h(r) - h_s\right| < \frac{\left(r^2 - R^2\right)^2}{r^3} \tag{18}$$

in which $\left|\lambda_{1,2}\right|$ denotes the maximum magnitude of the roots of the quadratic equation $P\lambda^2 - B\lambda + 1 = 0$, the roots being:

$$\lambda_1, \lambda_2 = \frac{B \pm \sqrt{B^2 - 4P}}{2P} \tag{19}$$

which are complex if $B^2 < 4P$. A complex root's magnitude is $\sqrt{\nu_{1,2}^2 + w_{1,2}^2}$ where $\lambda_{1,2} = \nu_{1,2} \pm w_{1,2} \cdot i$ (with $i^2 = -1$). Equation (18) imposes a rather stringent convergence condition of the series $F(h,r)$ in equation (17), especially in the limit $r \to R$.

The implementation of the implicit solution (17) requires choosing a value of r in the interval $[r_s, r_s + \delta]$, in which δ is a small increment of r. Next, the power series (17) is approximated by an expansion of order M, the functions $f_n(r)$, $0 \leq r \leq R$, are calculated, and the following polynomial equation on h is solved:

$$\sum_{n=0}^{M} \left(h(r) - h_s\right)^n f_n(r) \approx \frac{h_s^2}{2} \tag{20}$$

An estimate of $h(r)$ that satisfies equation (20) according to a user-specified closure criterion is taken as the solution $h(r)$. To ensure accuracy of the solution, the first choice of r, $r_1 = r_s + \delta$, must be quite close to r_s. The head h_s at r_s is used as guess to start the search for $h(r_1)$. When an estimate for the latter is obtained, it is used as a starting guess for the next head at $r_2 = r_1 + \delta$. This procedure is repeated for as many values of r as deemed adequate to characterize the phreatic surface in the neighbourhood upstream of r_s. To progress with the solution upstream beyond the vicinity of r_s, one must reset the downstream boundary to one of the calculated pairs (r, $h(r)$). That is, r_s becomes r and h_s becomes $h(r)$ in equations (10)–(17). The pair (r, $h(r)$) so established is used to reformulate equations (10)–(17) to continue solving for the hydraulic head upstream of the newly set boundary condition. This procedure is repeated until the upstream boundary is reached. This iterative solution procedure is known as analytic continuation and is a powerful tool in real- and complex-variable calculus (see further mathematical details in Needham, 1997, or Penrose, 2004, pp. 129–133). The polynomial equation (20) can be solved with numerical software such as Mathematica and Matlab, which feature symbolic operators to generate functions of type $f_n(r)$ (see equation (12)). It is recommended to use expansions of order $M \geq 5$ in equation (20).

THE CASE OF RECTANGULAR TRIBUTARY AQUIFER

This section is an abridged version of the approach by Loáiciga (2005), and it is included for comparison purposes with the results presented in the previous section. Focusing on Fig. 2, the relationship between the recharge accruing to groundwater and the discharge expressed by Darcy's law at a distance r from the origin requires that $-N(R - r)b = -Kb(h - rB)h'$, whose boundary condition is $h(0) = h_0$. Notice that groundwater discharge equals zero at $r = R$, where either $h = RB$ (that is, the saturated thickness is zero), or $h' = 0$. Letting $\alpha = K/N$ in the previous ODE one obtains $h'(r) = (R - r)/(\alpha h - r\alpha B) = (R - r)/z(r)$, in which $z(r) = \alpha h(r) - r\alpha B$ and $z'(r) = \alpha h' - \alpha B$. Replacing the expression for $h'(r)$ into the latter equation produces the following ODE:

$$z(r)\,z'(r) + \alpha\,B\,z(r) - \alpha \cdot (R - r) = 0 \tag{21}$$

Define the variable $u = R - r$. Thus, $z(r = R - u) \equiv \tilde{z}(u) = \alpha\,\tilde{h}(u) - (R - u)\,\alpha\,B$, where $\tilde{h}(u) = h(r = R - u)$. Let $y(u) = \tilde{z}(u)/\sqrt{\alpha}$. Using u and $y(u)$ in equation (21) yields the following equation (where $a = \sqrt{\alpha}\;\;B = \sqrt{K/N}\;\;B$):

$$y(u)\,y'(u) - a\;\;y(u) + u = 0 \qquad 0 \leq u \leq R \tag{22}$$

which is an Abel-type, nonlinear, ODE. Its boundary condition is:

$$y(R) = \frac{\alpha\,h(0)}{\sqrt{\alpha}} = \sqrt{\alpha}\;\;h_0 \tag{23}$$

An order-of-magnitude analysis of the flow parameter $a = \sqrt{K/N}\;\;B$ is warranted. The factor $\sqrt{K/N}$ typically ranges between 0.1 (when K = 0.001 m day^{-1} and N = 0.1 m day^{-1}) and 100 (when K = 10 m day^{-1}and N = 0.001 m day^{-1}) in perched aquifers. Limiting the aquifer slope to the range $0 < B = \tan\beta \leq 0.1$ bounds the flow parameter so that $0 < a \leq 10$, a meaningful range from a practical standpoint.

Upon solution of equations (22)–(23) for $y(u)$, the hydraulic head $h(r)$ is recovered by means of the following identity:

$$\widetilde{h}(u) = \frac{y(u)\sqrt{\alpha} + (R-u)\alpha B}{\alpha} = \frac{\widetilde{z}(u) + (R-u)\alpha B}{\alpha} = \frac{z(r) + r\alpha B}{\alpha} = h(r) \tag{24}$$

with $h(0) = h_0$.

Unlike the ODE (4) for radial discharge, equation (22) can be integrated in finite form. There are three solution pathways for the phreatic surface, corresponding to the cases $a = 2$, $a > 2$, and $a < 2$. This is a mathematical necessity. From a physical point of view, however, the phreatic surface varies continuously over the range of the flow parameter a (that is, over $a > 0$).

The case $a = 2$ produces the following implicit solution for $y(u)$:

$$\left|u - y(u)\right| \cdot e^{\frac{u}{u-y(u)}} = k_1 \tag{25}$$

in which $k_1$is a constant obtained from the boundary condition (23) for $y(R)$.

The case $a > 2$ produces the following implicit solution for $y(u)$:

$$\left|y(u) - v_1 \cdot u\right|^{v_1} \cdot k_2 = \left|y(u) - v_2 \cdot u\right|^{v_2} \tag{26}$$

in which $v_1 = (-a+\delta)/2, v_2 = (-a-\delta)/2$, where $\delta = (a^2-4)^{1/2}$, and k_2 is a constant calculable from the boundary condition (23).

Lastly, the case $a < 2$ produces the following implicit solution for $y(u)$:

$$\ln\left|u^2 + a\cdot u \cdot y(u) + y(u)^2\right| + \frac{2\,a}{\sqrt{4-a^2}} \cdot \operatorname{arctg}\left[\frac{2u + a\,y(u)}{y(u)\sqrt{4-a^2}}\right] = k_3 \tag{27}$$

In which “arctg” denotes the inverse tangent function, expressed in radians, and k_3 is an integration constant obtained from the boundary condition (23).

PERSPECTIVES ON THE RADIAL AND RECTANGULAR FLOW SOLUTIONS

The ODE (4) for bi-circular-sector discharge is mathematically more complex than that for rectangular-strip discharge in equation (21). This fact is reflected in the approximated and iterative nature of its solution by a truncated power series (equation (20)). It is fair to state that the bi-circular-sector problem is “more nonlinear” than the rectangular-strip one. In the latter case, a physically meaningful flow factor that ties hydraulic conductivity, recharge and bedrock slope controls the solution pathway, of which there are three possible ones, all of them expressible in terms of combinations of elementary functions and the downstream boundary condition.

One common theme to the ODEs (4) and (21) is that their hydraulic heads at the headwater, $h(R)$, may either equal the elevation of the aquifer–bedrock boundary (= RB), in which the saturated thickness of groundwater flow is zero, or have a gradient $h'(R) = 0$. These two conditions force zero discharge at the headwater, and all the recharge drains through the downstream end of the aquifer. Yet, it is plausible that when the aquifer–bedrock boundary’s slope is very mild and/or the recharge over conductivity ratio sufficiently large, there may be mounding of the phreatic surface and the recharge may drain through both the downstream and upstream boundaries of the sloping aquifer. The ODE for flow in a bi-circular sector with specified upstream flow $q(R)$ (in the direction of increasing r) is a slightly modified version of equation (4):

$$r\,h\,h' - r^2\,B\,h' + P\,r^2 - P\,R^2 + \frac{q(R)}{K\cdot\theta} = 0 \tag{28}$$

The solution of the ODE (28) is arrived at with methodology analogous to that presented in equations (7)–(17) after proper consideration is given to the rightmost (constant) term on the left-hand side of the equation.

In comparing the solutions for $h(r)$ stemming from bi-circular sectors and rectangular strips, it is desirable that their discharges per unit length of downstream boundary be the same for either geometric configuration. In other words (see Figs 1 and 2 to review the involved geometries):

$$\frac{N\cdot R\cdot b}{b} = \frac{N\cdot\left(\dfrac{R^2 - r_s^{\,2}}{2}\right)}{r_s} \tag{29}$$

in which the left-hand and right-hand sides represent the unit discharges in the rectangular strip and bi-circular sectors, respectively. Solving for the offset distance r_s yields:

$$r_s = \left(\sqrt{2} - 1\right)R \approx 0.414R \tag{30}$$

which fixes r_s to produce equal unit downstream discharges for given R and any rectangular width b. Equation (30) shall prove useful in the next section dealing with a computational example.

COMPUTATIONAL EXAMPLE

The effect of aquifer slope on the phreatic surface

The effect of the slope of the aquifer–bedrock boundary (B) on the phreatic elevation $h(r)$ in a bi-circular sector is illustrated in Figs 3 and 4. The hydraulic ratio is $P = N/(2K) = 10^{-3}/(2 \times 1) = 5 \times 10^{-4}$, where N and K are in m day^{-1}; $R = 1000$ m, and $r_s = \sqrt{2} - 1 \approx 0.414R$ in both figures. The radial offset r_s was chosen so that the unit downstream discharge in the bi-circular sector is equal to the unit discharge from a rectangular strip of length $R = 1000$ m and width b (see Fig. 2, equation (32)). The head $h_s = r_sB + 2$ m so that the downstream saturated thickness equals 2 m in Figs 3–4.

Figure 3 corresponds to the case of steeper slope $B = 0.1$. It is seen there that the hydraulic head $h(r = R)$ equals the bedrock elevation $RB = 100$ m at the upstream boundary, for a saturated thickness equal to zero at $r = R$, implying nil groundwater flow there. The saturated thickness (= $h(r) - rB$) increases with decreasing distance from the origin up to a distance of about $0.48R$. Thereafter, the saturated thickness decreases (while the hydraulic gradient increases) towards $r = r_s$ to achieve its downstream value equal to 2 m. The groundwater velocity $v(r) = K\cdot h'(r)$ varies throughout the flow length, being controlled by the hydraulic-head gradient, which is seen to be largest as the downstream boundary is approached.

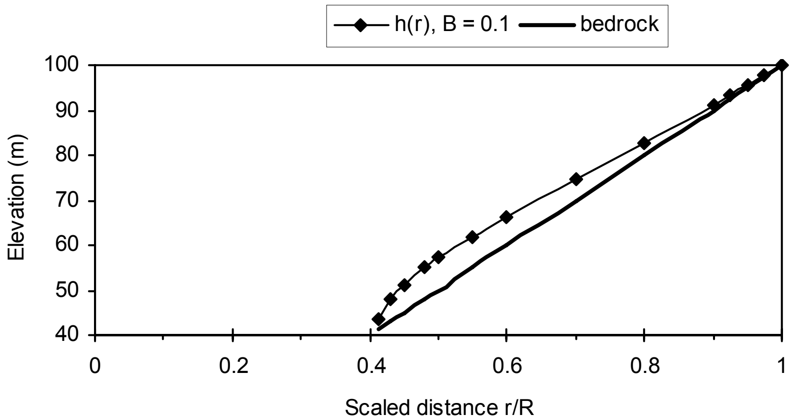

Fig. 3 Calculated phreatic surface ($h(r)$) in a bi-circular sector; hydraulic ratio $P = 5 \times 10^{-4}$, slope of the aquifer–bedrock boundary $B = 0.1$; $R = 1000$ m; the sector starts at $r_s = 0.414R$; downstream head $h_s = r_sB + 2$ m. See text for details.

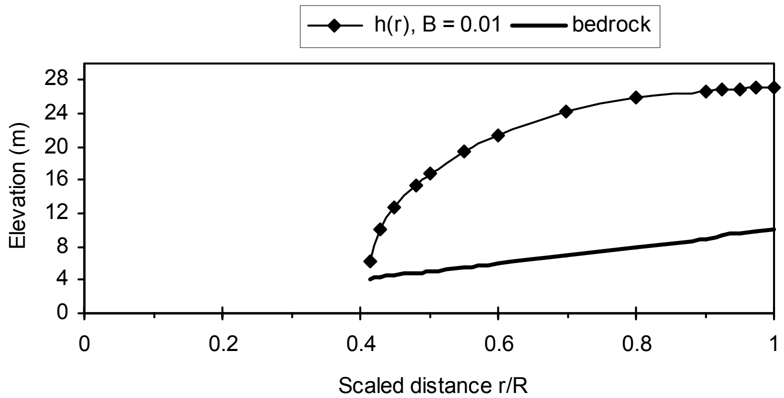

Fig. 4 Calculated phreatic surface ($h(r)$) in a bi-circular sector; hydraulic ratio $P = 5 \times 10^{-4}$, slope of the aquifer–bedrock boundary $B = 0.01$; $R = 1000$ m; the sector starts at $r_s = 0.414R$; downstream head $h_s = r_sB + 2$ m. See text for details.

Figure 4 displays the calculated hydraulic head in a bi-circular sector for the case of an aquifer–bedrock slope $B = 0.01$, the mildest of the two considered in this example. Other input variables and parameters are the same as those used in Fig. 3. There is clear departure in the geometry of the phreatic surface depicted in Fig. 4 relative to that observed in Fig. 3, which features a steeper slope. The saturated thickness equals 17.1 m at $r = R$, the upstream boundary, and achieves a maximum near $r = 0.85R$, with a minimum equal to 2 m at the downstream boundary. The considerable saturated thickness observed throughout the aquifer in Fig. 4—much larger than that in Fig. 3—is necessary to convey groundwater discharge over a relatively mild slope. The hydraulic-head gradient is zero at the upstream boundary, a necessity imposed by the zero-discharge condition at that location. The hydraulic-head gradient increases with decreasing distance from the origin to reach a maximum at the downstream boundary, where the saturated thickness is equal to 2 m (the same as in Fig. 3). Evidently, the groundwater velocity increases—driven by a steeper hydraulic gradient—as the downstream boundary is approached.

The effect of hydraulic conductivity on the phreatic surface

Figure 5 shows the effect of hydraulic conductivity on the phreatic surface, all other factors kept constant. The slope of the aquifer–bedrock boundary is B = 0.01. Phreatic surfaces were calculated for (a) a hydraulic conductivity K = 1 m day^{-1} and hydraulic ratio $P = N/(2K) = 10^{-3}/(2 \times 1) = 5 \times 10^{-4}$ (already shown in Fig. 4), and (b) K = 50 m day^{-1}, with $P = N/(2K) = 10^{-3}/(2 \times 50) = 10^{-5}$. The top curve in Fig. 5 shows the calculated hydraulic head (h) for K = 1 m day^{-1}. The middle curve is the hydraulic head corresponding to K = 50 m day^{-1}. The bottom curve is the aquifer–bedrock boundary. It is clear from Fig. 5 that the five-fold rise in hydraulic conductivity reduces the saturated thickness substantially, from 17.1 m to 0 m at $r = R$, for example, as the hydraulic conductivity rises from 1 to 50 m day^{-1}. This is due to greater groundwater velocities and associated reduction of saturated thickness needed to drain the same amount of groundwater flow.

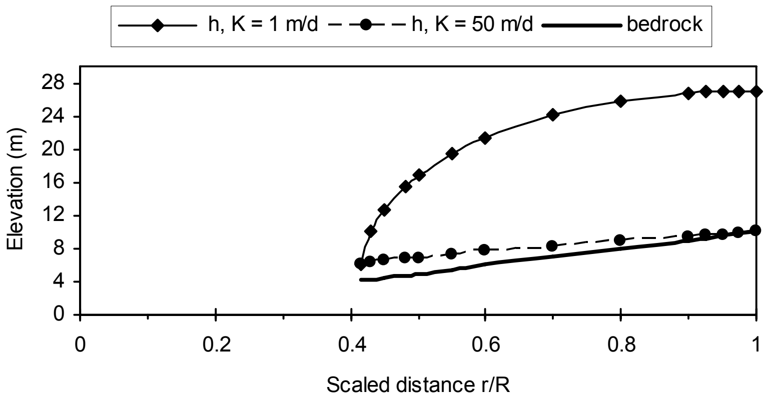

Fig. 5 Calculated phreatic surface ($h(r)$) in a bi-circular sector; slope of the aquifer–bedrock boundary B = 0.01; R = 1000 m; the sector starts at $r_s = 0.414R$; downstream head $h_s = r_sB + 2$ m. The top curve corresponds to a hydraulic ratio $P = 5 \times 10^{-4}$ with K = 1 m day^{-1}. The middle curve corresponds to a hydraulic ratio $P = 10^{-5}$ with K = 50 m day^{-1}. See text for details.

Comparison of bi-circular and rectangular-strip phreatic surfaces

Figure 6 shows the computed hydraulic head $h(r)$ in a rectangular strip and bi-circular sector. The former is R = 1000-m-long, while the latter spans from $r_s = 0.414R$ (see equation (32)) to $r = R$. Both aquifers discharge the same flow of groundwater per unit length of downstream boundary (= NR). The aquifer–bedrock boundary's slope equals B = 0.06325. This choice of slope renders the flow parameter a equal to 2, which is the value of the bifurcation threshold in the case of a rectangular-strip aquifer. In addition, K = 1 m day^{-1}, and $N = 10^{-3}$ m day^{-1} for both aquifer geometries. The hydraulic ratio $P = N/(2K) = 5 \times 10^{-4}$ and the flow factor $a = \sqrt{K/N}\ B = 2$ in the bi-circular sector and rectangular strip, respectively. It is seen in Fig. 6 that the rectangular strip requires a longer flow length and relatively larger saturated thickness for $r/R < 0.6$, approximately, relative to the bi-circular sector. The rectangular strip exhibits smaller hydraulic-head gradients than the bi-circular sector, thus supporting lower groundwater velocities for the stated conditions.

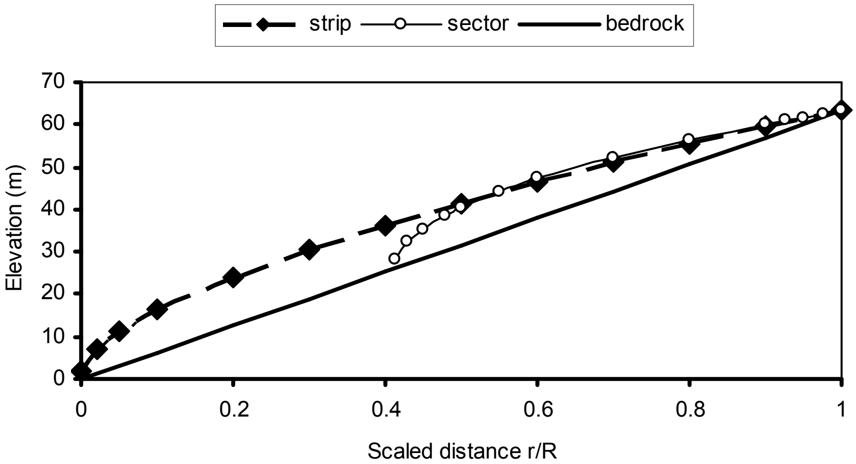

Fig. 6 Calculated phreatic surface ($h(r)$) in a rectangular strip and in a bi-circular sector. Slope of the aquifer–bedrock boundary B = 0.06325; R = 1000 m; downstream saturated thickness = 2 m in both cases. The sector starts at r_s = 0.414R. The hydraulic ratio $P = 5 \times 10^{-4}$ for the sector, while the flow factor a = 2 for the strip, both with K = 1 m day^{-1} and $N = 10^{-3}$ m day^{-1}. The unit discharge through the downstream boundaries of the strip and sector is the same (= NR).

CONCLUSION

An implicit solution was developed for the geometry of the steady-state phreatic surface in a sloping unconfined aquifer with bi-circular sectorial (planar) geometry. This aquifer geometry conforms to radially convergent groundwater flow towards a downstream boundary (lake or stream) with constant water level. The implicit solution allowed investigation of the role of hydraulic characteristics (recharge, hydraulic conductivity) and geometry (slope, flow length, radial convergence) on the shape of the steady-phreatic surface with constant-head downstream boundary. In addition, results for the radially convergent groundwater flow were compared with those of the previously solved rectangular sloping aquifer.

The presented solutions for steady-state phreatic surfaces in sloping aquifers are of practical value from hydrological and geotechnical perspectives. Inferences concerning the height of saturation, groundwater velocities (from Darcy's law), flow accumulation, pore-pressures, and aquifer–stream or aquifer–lake interactions can be improved with the aid of the derived analytical solutions.

REFERENCES

Abel, N. H. (1839) *Oeuvres Complètes*, vol. II, 236–245, Oslo, Norway.

Cherkauer, D. S. & Ansari, S. A. (2005) Estimating groundwater recharge from topography, hydrogeology, and land cover. *Groundwater* **43**, 102–112.

Coduto, D. P. (1999) *Geotechnical Engineering: Principles and Practices.* Prentice Hall, New Jersey, USA.

Dunne, T. (1990) Hydrology, mechanics, and geomorphic implications of erosion by surface flow. In: *Groundwater Geomorphology: the Role of Subsurface Water in Earth-Surface Process and Landforms*, Special Paper Geological Society of America 252, 1–28.

Kamke, E. (1959) *Methods of Solutions and Solutions of Differential Equations* (fourth edn), Chelsea Publishing Co., New York, USA.

Loáiciga, H. A. (2005) Steady-state phreatic surfaces in sloping aquifers. *Water Resour. Res.* **41**, W08402, doi:10.1029/2004WR003861.

Loáiciga, H. A. & Huang, A. (2005) Flooding-cycle analysis in wetlands with negligible overland drainage. In: *Dynamics and Biogeochemistry of River Corridors and Wetlands*, 122–129. IAHS Publ. 294, IAHS Press, Wallingford, UK.

Needham, T. (1997) *Visual Complex Analysis*. Clarendon Press, Oxford University, Press, Oxford, UK.

Penrose, R. (2004) *The Road to Reality*. Alfred A. Knoff Inc., New York, USA.

Philip, J. R. (1993) Variable-head ponded infiltration under constant or variable rainfall. *Water Resour. Res.* **29**, 2155–2165.

Polubarinova-Kochina, P. Y. (1962) *Theory of Groundwater Movement*. Princeton University Press, New Jersey, USA.

Polyanin, A. D. & Zaitsev, V. F. (1995) *Handbook of Exact Solutions for Ordinary Differential Equations.* CRC Press, Boca Raton, Florida, USA.

Smith, R. E. (2002) Infiltration theory for hydrologic applications. *Water Resources Monograph 15*, American Geophysical Union, Washington, DC, USA.

Terzaghi, K., Peck, R. B. & Mesri, G. (1996) *Soil Mechanics in Engineering Practice.* John Wiley & Sons Inc., New York, USA.

Received 21 April 2006; accepted 11 March 2006